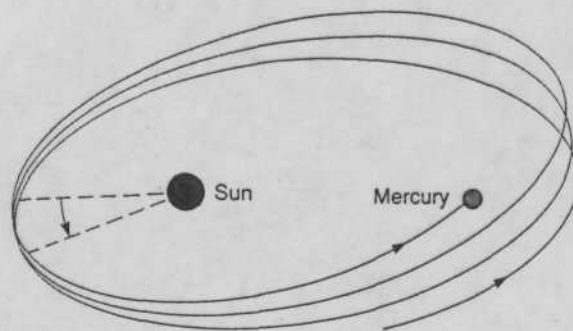


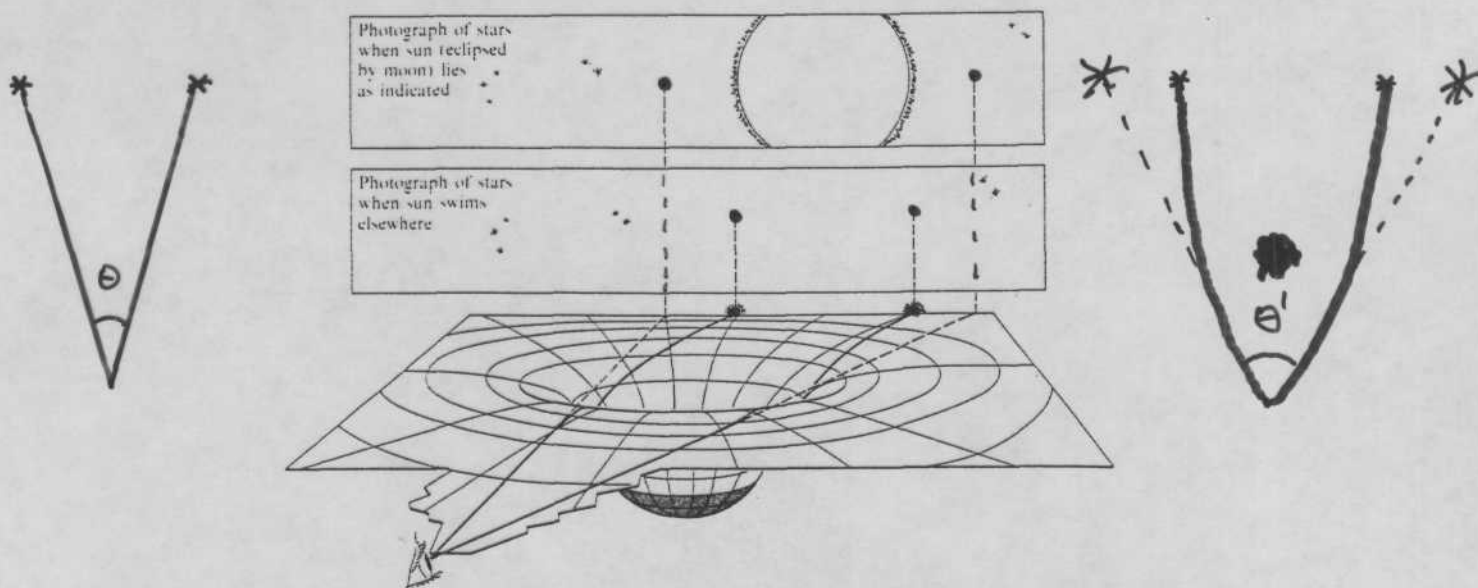
1. Закон Ньютона.
2. Прцессия перигелия Меркурия.
3. Отклонение лучей света в гравита-м поле.
4. Задержка радиосигналов.
5. Красное смещение.
6. Гравитационные волны
7. Чёрные дыры.

# Приращение перигелия Меркурия.

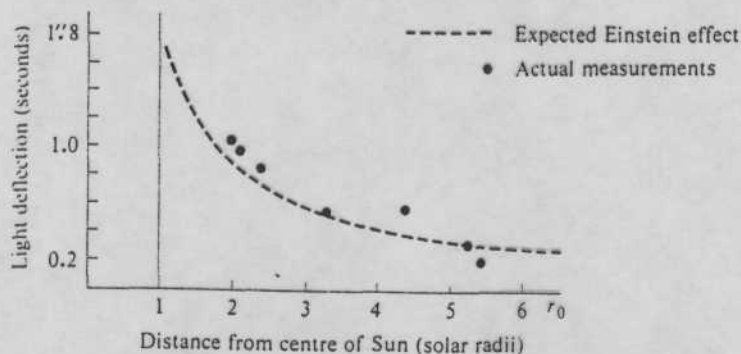


Perihelion advance of Mercury. The point of closest approach of Mercury to the Sun, the perihelion, advances by about 574" per century. Of this, 531" are caused by gravitational perturbations from the other planets, primarily Venus, Earth and Jupiter. The difference, 43" per century, was accounted for by general relativity.

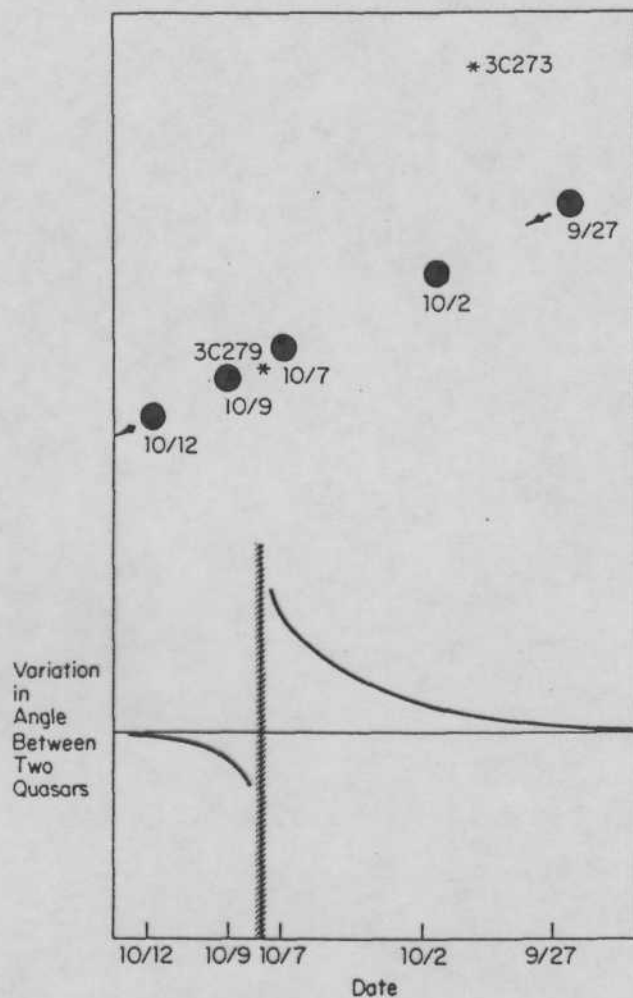
# Отклонение света в гравитационном поле ⊙



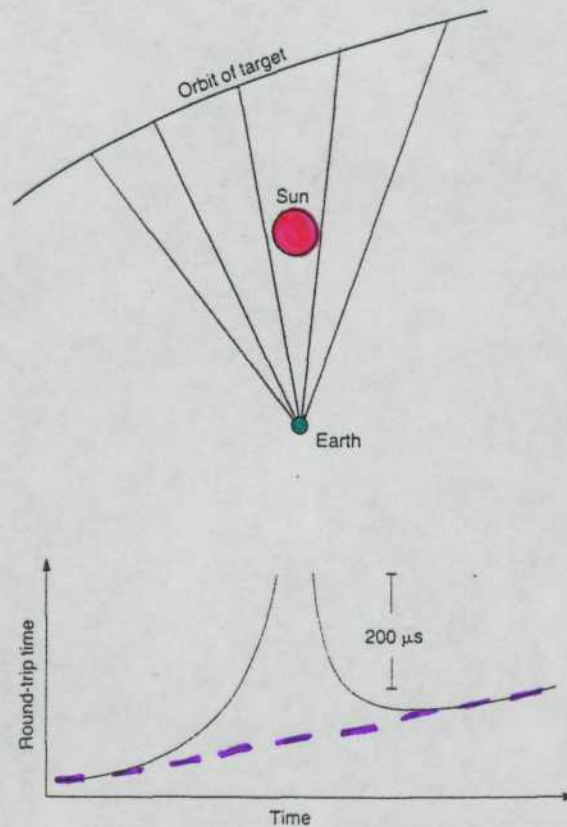
Bending of light by the Sun depicted as a consequence of the curvature of space near the Sun. The ray of light pursues geodesic, but the geometry in which it travels is curved (actual travel takes place in space-time rather than space; the correct deflection is twice that given by above elementary picture). Deflection inversely proportional to angular separation between star and centre of Sun.



Eddington's results from the 1919 eclipse expedition, showing a close correlation with Einstein's theory.



Quasar light deflection measurements. The upper portion of the diagram shows the two quasars 3C273 and 3C279, and the apparent path of the Sun. The lower portion shows the angular variation between the two quasars as the Sun passes in front of 3C279. This variation is due to the deflection of light from 3C279 by the Sun.



The time delay of light. A target such as planet or a spacecraft moves from left to right on the far side of the Sun while periodic radar tracking signals are sent to it from Earth. As the signals pass the Sun at close range, they suffer an additional delay of up to several hundred microseconds over and above the expected round-trip travel time, which for Mars would be around 42 minutes. Shown in the lower half of the figure is a schematic (and exaggerated) plot of the observed round-trip travel time as a function of time, showing the excess delay for rays that pass near the Sun.



Проверка ОТО  
в слабых полях  
в системе Луна-Земля

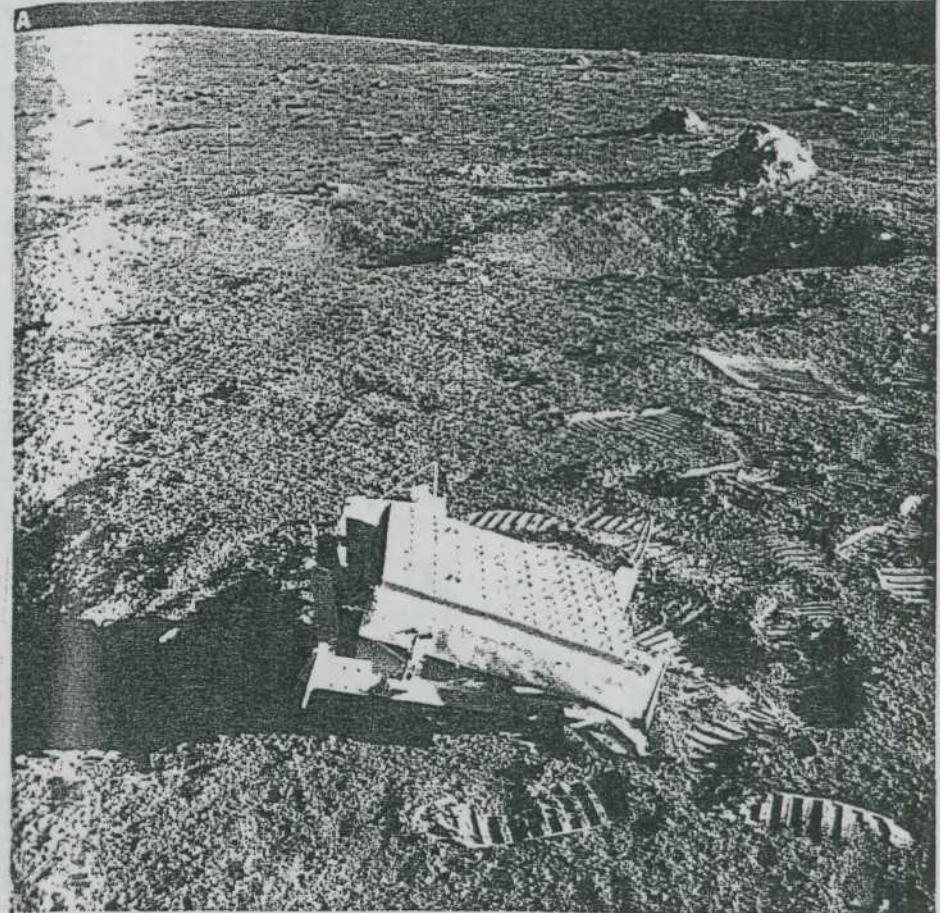
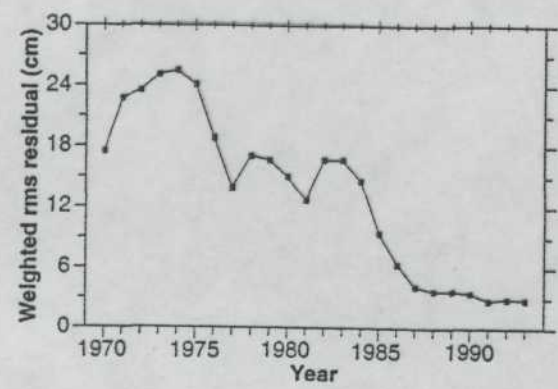


Fig. 1. (A) Photograph of a retroreflector array of Apollo 14 on the lunar surface. (B) Geographical distribution of the retroreflector arrays on the lunar surface. The labels A-11, A-14, and A-15 denote the Apollo 11, 14, and 15 sites, respectively, whereas L-1 and L-2 indicate the Lunakhod 1 and 2 locations (no returns are available from Lunakhod 1).

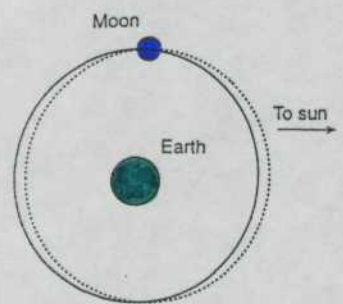
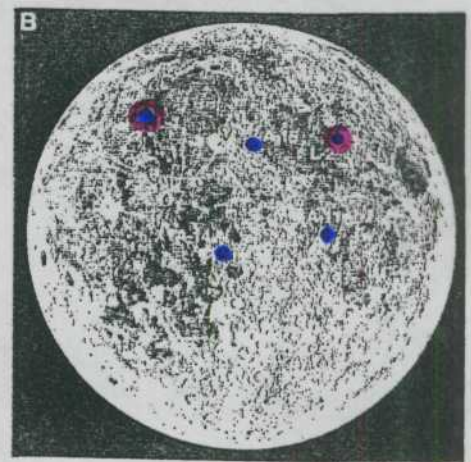


Fig. 4. Lunar orbit about the Earth as affected by the Nordtvedt term. A violation of the Equivalence Principle would cause the orbit of the moon about the Earth-moon center of mass to be polarized in the direction of the sun, with a characteristic size of  $\sim 13$  m. The solid line represents the lunar orbit in General Relativity, and the dotted line represents the lunar orbit if the  $M_G/M_I$  values for the Earth and moon differ.

$$\left(\frac{\Delta a}{a}\right)_{\text{Луна-Земля}} = (-3.2 \pm 4.6) \times 10^{-13}$$



J.O. Dickey et al, Science, 265, 482 (94).

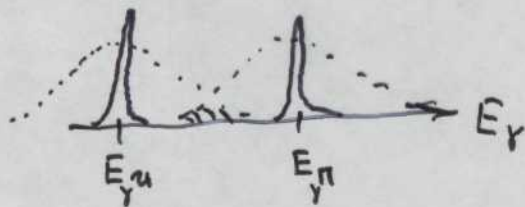


# Гравитационное красное смещение:

Эффект Мессбауэра.

$$\longleftrightarrow \gamma (10 \div 100) \text{ кэВ.}$$

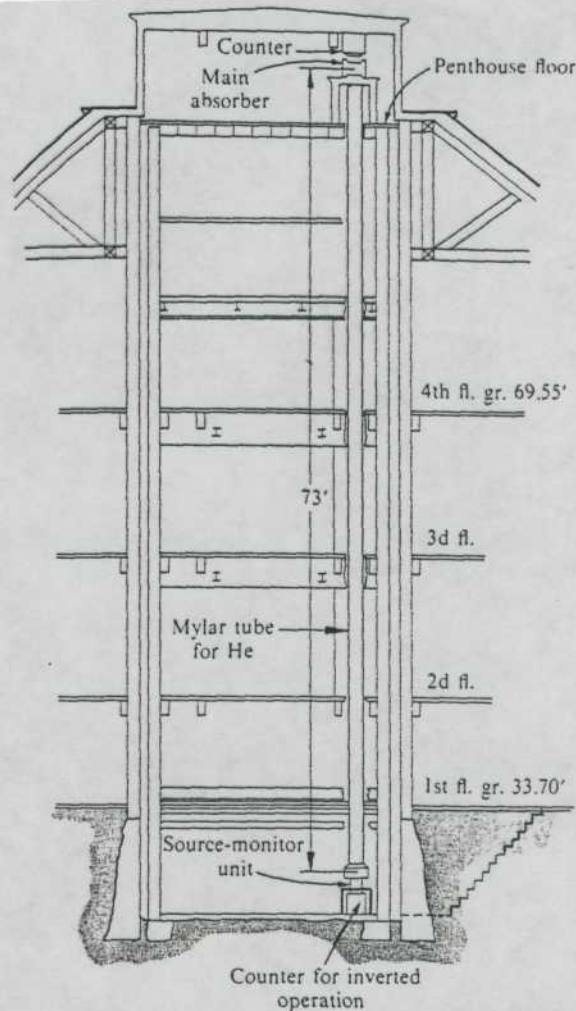
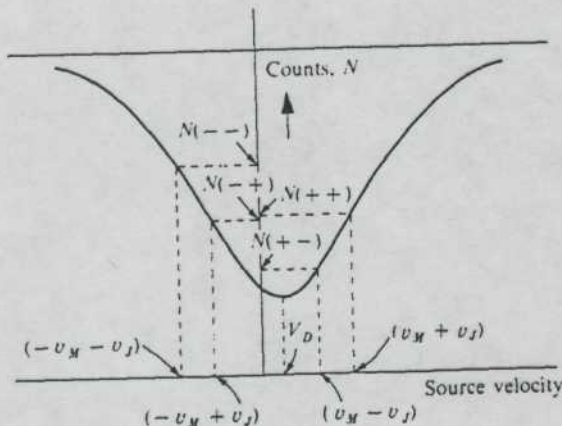
резонансное поглощение:



$$\sim 10^8 \text{ кГц} \rightarrow \gamma$$

$^{57}\text{Fe} : \Gamma/E_{\gamma} \approx 3 \cdot 10^{-13}$   
 $\Gamma \sim 10^{-9} \text{ эВ}$

$^{67}\text{Zn} : \Gamma \sim 5 \cdot 10^{-11} \text{ эВ}$   
 $\Gamma/E_{\gamma} \approx 5 \cdot 10^{-16}$



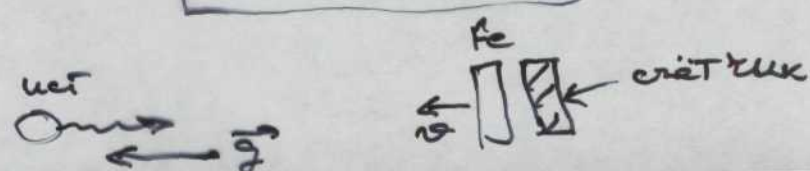
The experiment of Pound and Rebka (1959) and Pound and Snider (1965) on the gravitational red shift of photons rising 22.5 m against gravity through a helium-filled tube in a shaft in the Jefferson Physical Laboratory of Harvard University. The source of  $\text{Co}^{57}$  had an initial strength greater than a curie. The 14.4 keV gamma-rays had to pass in through an absorber enriched in  $\text{Fe}^{57}$  to reach the large-window proportional counters. Both source and absorber were placed in temperature-regulated ovens. The velocity of the source consisted of two parts: one steady ( $v_M$ ), to put the centre of the emission line on the part of the transmission curve that is nearly straight; and the other alternating between  $+v_J$  and  $-v_J$ , to sweep the transmission curve in this straight region; similarly when the steady velocity was  $-v_M$ . The departure from symmetry between the two cases  $+v_M$  and  $-v_M$  allows one to determine the offset  $V_D$  (the effect of gravitational red shift) from the zero-gravity case of stationary emitter and stationary absorber. The final result for the red shift was  $(0.9990 \pm 0.0076)$  times the value  $4.905 \times 10^{-15}$  of  $2gh/c^2$  predicted from the principle of equivalence (the difference between 'up' experiment and 'down' experiment).

$$m = E_{\gamma}/c^2$$

$$\Delta E = \frac{E_{\gamma}}{c^2} gh$$

$h = 22.5 \text{ m}, \quad \frac{\Delta E}{E} = gh/c^2 = 10^{-16}$

$$v \sim 1 \text{ мм/с}$$



# Гравитационные волны.

Наряду с СВ и РВ гравитационные откроют новые воз-ти.

РВ - квазары, пульсары, РИ, открытие ГВ...

## Отличия РВ и ГВ.

РВ

распро-ся в прост-ве

излуч-ся атомами  
и молекулами

$\lambda_{изл} \ll \lambda_{ист}$

Солнцное излучение

$$f \approx 10^7 - (10^{20}) \text{ Гц}$$

ГВ

изменение геометрии про-ва

увеличение  $\gg$  масс

$\lambda_{изл} \geq \lambda_{ист}$

отсутствие...

$$f \leq 10^4 - (10^{-20}) \text{ Гц}$$

$\Rightarrow$  разная информация о Вселенной

## Оценка частоты ГВ

$$R_g \approx \frac{2GM}{c^2} ; \quad \tau \approx \frac{2\pi R_g}{c} ; \quad f \sim \frac{1}{\tau}$$

$$f \leq \frac{1}{4\pi GM/c^3} \sim 10^4 \cdot \frac{M_{\odot}}{M} [\text{Гц}]$$



$$\underline{f = (1 \div 10^4) \text{ Гц}}$$

Источники: коллапс звезд  $\rightarrow$  НЗ, ЧД, колыбельная фаза  
эволюции 2<sup>х</sup> систем НЗ-ЧД, НЗ-НЗ.

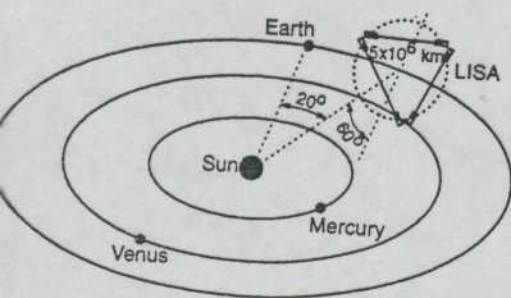
способ регистрации: резонансные антенны,  
(наземный) лазерные интерферометры.

$$\underline{f = (10^{-4} \div 1) \text{ Гц}}$$

источники: 2<sup>ые</sup> системы НЗ-НЗ, БК-БК, ЧД-ЧД.

способ регистрации: доплеровское мониторирование  
(космическое базирование) спутников, космические  
интерферометры, (2015г)

ограничения: давление солнечного ветра на спутник,  
световое давление, космические мусоры



$$\underline{f = (10^{-7} \div 10^{-9}) \text{ Гц}}$$

$$M \approx 10^{11} \cdot M_{\odot}$$

источники: ядра галактик, галактики и их скопления

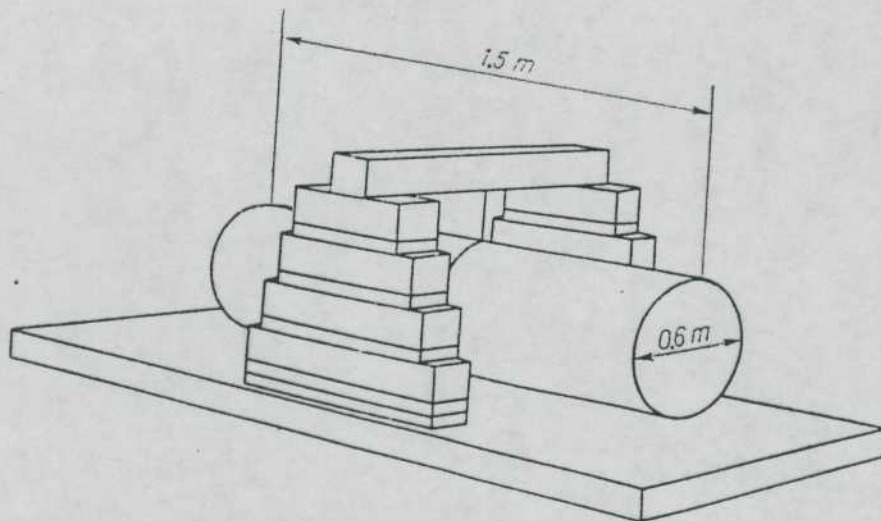
способ регистрации: измерение частоты мс пульсаров  
от времени ( $N \approx 10 \div 100$ ) в нескольких  
точках на Земле  
(изменение скорости хода часов)



# Эксперименты по поиску гравитационных волн.

20

Weber, 1961 г. ;  $\frac{\Delta l}{l} \approx 10^{-10}$  ,  $\Delta l \approx 10^{-8}$  см.  
 $f \sim 10^3$  Гц.



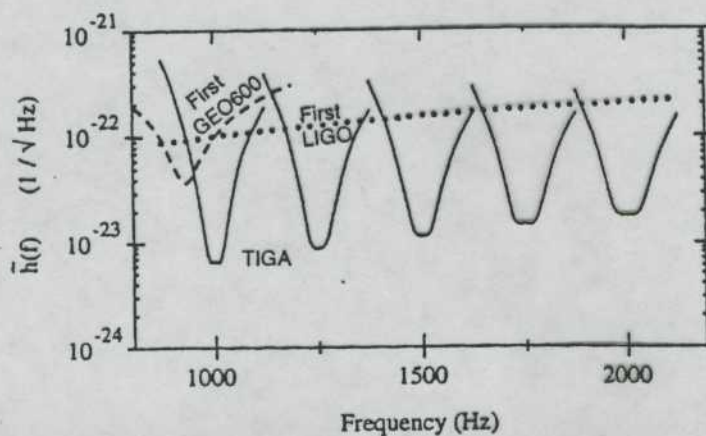
Weber's gravitational antenna. An aluminium cylinder is suspended from a metal frame resting on shock absorbers. The whole is placed on a metal foundation (adapted from Weber, 1961).

1995 г. NAUTILUS ,  $M = 3$  тонны ,  $T = 0.05$  К !

(цилиндры)  $\frac{\Delta l}{l} \approx 3 \cdot 5 \cdot 10^{-20}$ .

2005-2010 гг. TIGA ,  $M \approx 3, 5, 7, 13, 25$  тонн ,  $T \approx 0.05$  К

(сферы)  $\frac{\Delta l}{l} \approx 10^{-21}$



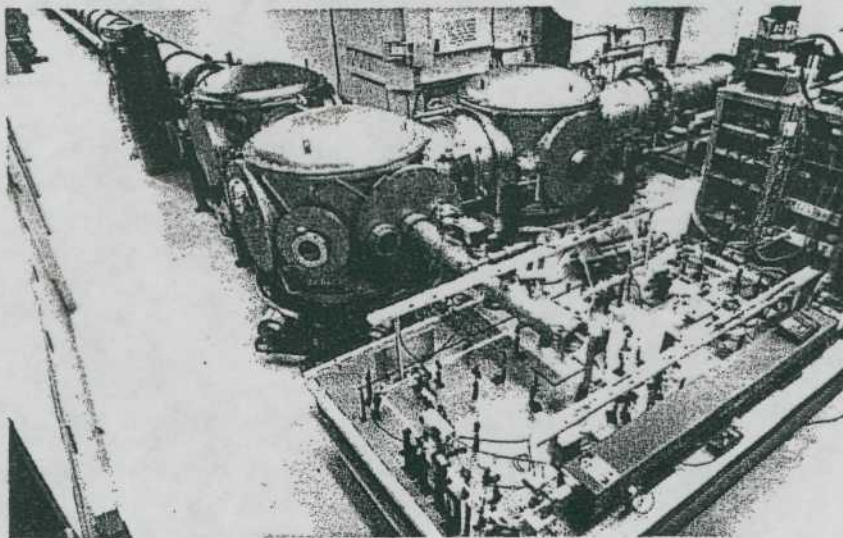


Figure 4: The LIGO Project's 40-meter "Mark II" prototype interferometer at Caltech. This prototype went into operation in 1993. It has much larger vacuum chambers, to accommodate bigger and better seismic isolation stacks, than those of the previous "Mark I" prototype (which operated from the early 1980s to 1992). [Courtesy the LIGO Project.]

$$\frac{\Delta l}{l} \approx 10^{-21} \Rightarrow \Delta l \approx 10^{-16} \text{ cm} \quad (\text{Roz} \cdot 10^{-3})$$

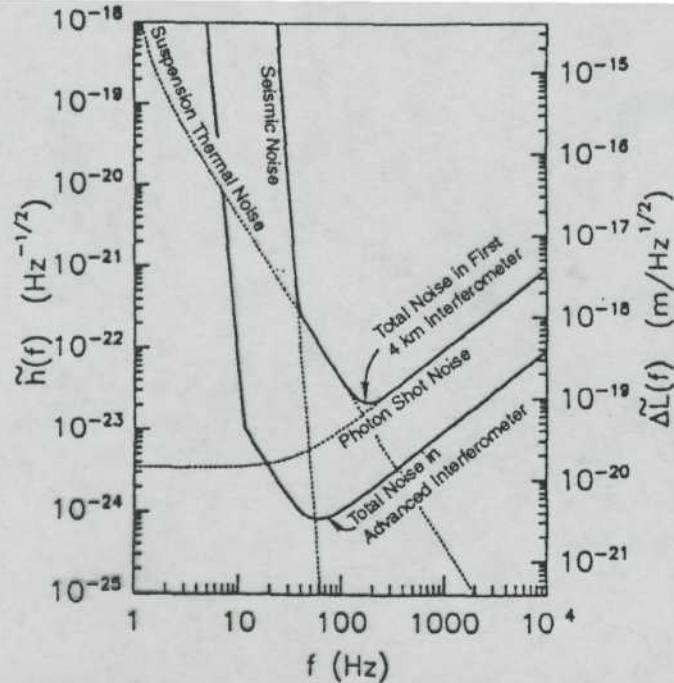
$$\Delta \theta \approx (0.3 \div 1)^\circ \text{ для } 2^\times \text{ и } 3^\times \text{ приборов}$$

$$\lambda^{\text{лазера}} \sim 10^{-4} \text{ cm}, \quad \Delta l \ll \lambda \Rightarrow \text{огромная интер-ть лазера}$$

$$W_{\text{лаз}} = 100 \text{ Вт} \Rightarrow \text{нагрев и т.д.}$$

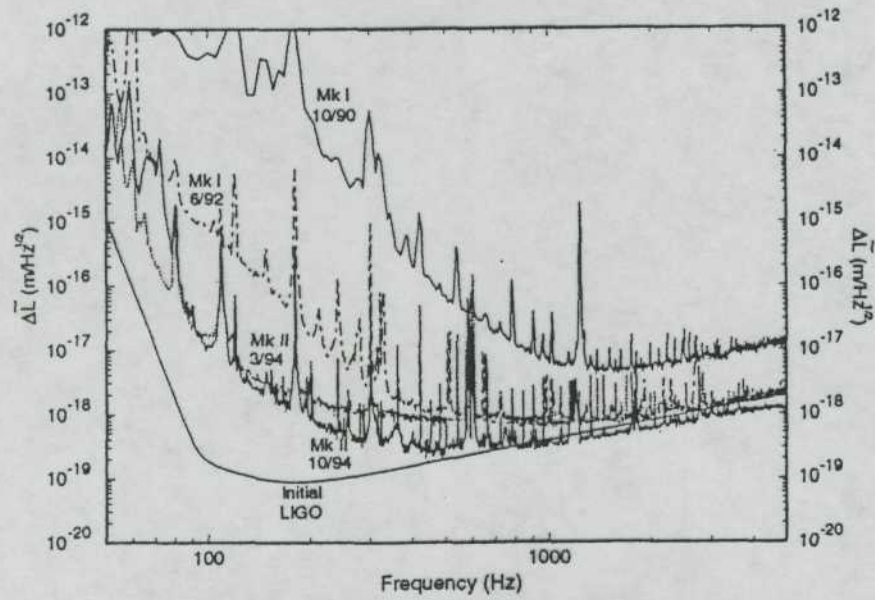






Сейсмический шум  
возбуждается при  
анализе сигналов  
с детекторов, расно-  
стояния  $\gg L$ .

The expected noise spectrum in each of LIGO's first 4-km interferometers (upper solid curve) and in more advanced interferometers (lower solid curve). The dashed curves show various contributions to the first interferometers' noise. Plotted horizontally is gravity wave frequency  $f$ ; plotted vertically is  $\tilde{h}(f)$ , the square root of the spectral density of the detector's output  $h(t) = \Delta L(t)/L$  in the absence of a gravity wave. The rms  $h$  noise in a bandwidth  $\Delta f$  at frequency  $f$  is  $h_{\text{rms}} = \tilde{h}(f) \sqrt{\Delta f}$ . (From Ref. [14].)



Measured noise spectra in the Caltech 40-meter prototype interferometer (Fig. 4). Since this prototype is devoted to learning to control displacement noise, the spectra shown are  $\Delta \tilde{L}(f)$ , the square root of the spectral density of the measured arm-length difference. Each of the many spectral lines is well understood, and most could be removed if their removal were of high priority (e.g., they are multiples of the 60 Hz line frequency sneaking into the apparatus by known routes). Those few, very narrow lines that cannot be physically removed by cleaning up the instrument (e.g., thermally-driven violin-mode resonances of the wires that suspend the test masses) will be filtered out in the data analysis. Thus, the interferometer sensitivity is characterized by the continuum noise floor and not the lines. (From Ref. [18].)



## Сложности ...

(23)

LIGO:  $\Delta l \sim 10^{-16} \text{ см}$ ,  $\lambda_{\text{лаз}} \sim 10^{-4} \text{ см}$

$$\frac{\Delta l}{\lambda} \approx 10^{-12} \quad !!!$$

как можно такое наблюдать?!

- 1)  $f = 10^2 \text{ Гц}$   $L \approx 4 \text{ км} \Rightarrow \text{за } T/2 \leftrightarrow \text{свет } 100 \text{ раз}$



Каждый разгиб уве-св в  $10^2 \text{ раз}$   $\times 2$  для  $2^x$  раз

$$\Delta \varphi \sim 100 \times 2 \times 2\pi \frac{\Delta l}{\lambda} \sim 10^{-9}$$

$$S(\Delta \varphi) \sim \frac{1}{\sqrt{N_g}} \Rightarrow N_g \approx 10^{18} / 0.01 \text{ с}$$

$$\Rightarrow W = 100 \text{ Вт} ! \text{ непрерывный режим}$$

$$\text{Зеркала } R \rightarrow \frac{1}{20} \rightarrow 5 \text{ Вт}$$

- 2. Тепловое движение молекул:  $\Delta l_{\text{rms}} = \sqrt{\frac{kT}{m\omega}} \approx 10^{-10} \text{ см}$   
( $\Delta l \approx 10^{-16} \text{ см}$ )  $\omega \sim 10^{14} \text{ с}^{-1}$

решение:  $\varnothing \text{ луча} = 5 \text{ см} \Rightarrow \text{усреднение по } \sim 10^{17} \text{ атомов}$

$$\tau_{\text{уср}} \approx 0.01 \text{ с} \Rightarrow 10^{11} \text{ колебаний атома}$$

- 3. Сейсмические колебания:

$$\Delta l_{\text{сей}} \approx 10^{-8} \text{ см} \left( \frac{100 \text{ Гц}}{f} \right)^{3/2}$$

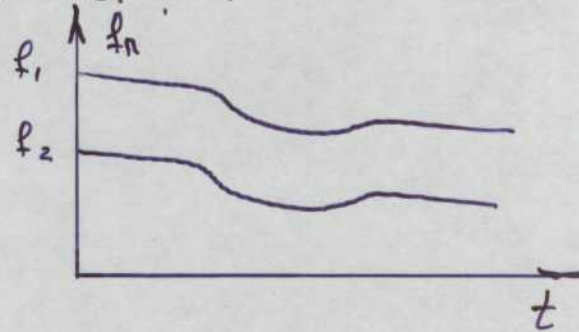
интерферометры разнесены в США и Европе.

# Обнаружение корреляций в изменении гравитации Пути-6

$$\varepsilon_{\text{наб}} \begin{cases} f \sim 10^{-7} \text{ } \mu\text{г}; & \tau \sim 10^{-7} \cdot \pi \cdot 10^7 \text{ сек } \left( \frac{1}{10 \pm 5} \right) = \text{неск-0 мкс} \\ f \sim 10^{-9} \text{ } \mu\text{г}; & \tau \sim 10 \pm 20 \text{ лет} \end{cases} !$$

измерения уже ведутся.

$$f = (10^{-15} \div 10^{-18}) \text{ } \mu\text{г}$$



$$\lambda \sim R_{\text{вселенной}}$$

способ регистрации: квазирезонансная компонента РИ.  
(См. - на СОВЕ.)

## лазерный интерферометр

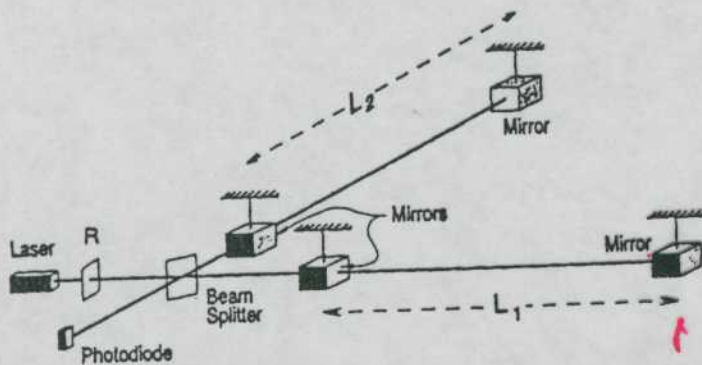


Figure 2: Schematic diagram of a laser interferometer gravitational wave detector. (From Ref. [14].)

$$L_1 \sim L_2 \sim L \sim 1 \text{ км}$$

технология отра-ся  
уже в течение 25 лет!

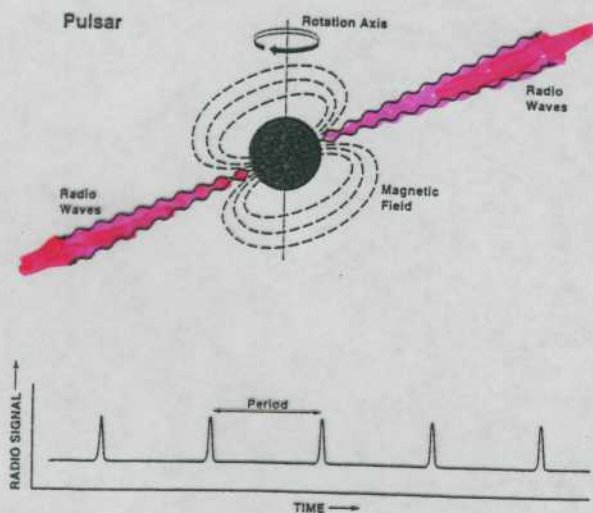
VIRGO ;  $L \approx 3 \text{ км}$  1 мт в Европе, 2003 год.

LIGO ;  $L \approx 4 \text{ км}$  , 2 мт в US, 2001 год



# Обнаружение гравитационных волн

25



Нейтронные звёзды.

$$\phi = 10-30 \text{ км}$$

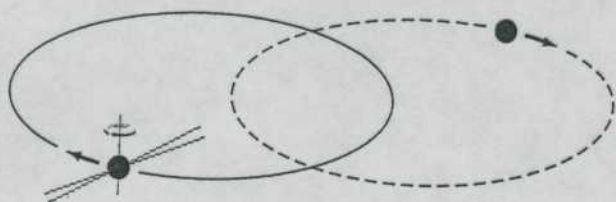
$$M \approx 1 \times M_{\odot}$$

$$R \approx R_{\text{ядра}}$$

$$B \approx 1 \div 50 \text{ МРс}$$

$$T_{\text{вращения}} \approx 2 \div 2000 \text{ мсек.}$$

Двойные системы НЗ.  
(проверка ОТО в сильных полях)



PSR 1913+16

$$M_1 = 1.50^{+0.26}_{-0.14}, M_2 = 0.258^{+0.028}_{-0.016}$$

$$T_{\text{орб}} \approx 7.8 \text{ часа}$$

$$e = 0.62$$

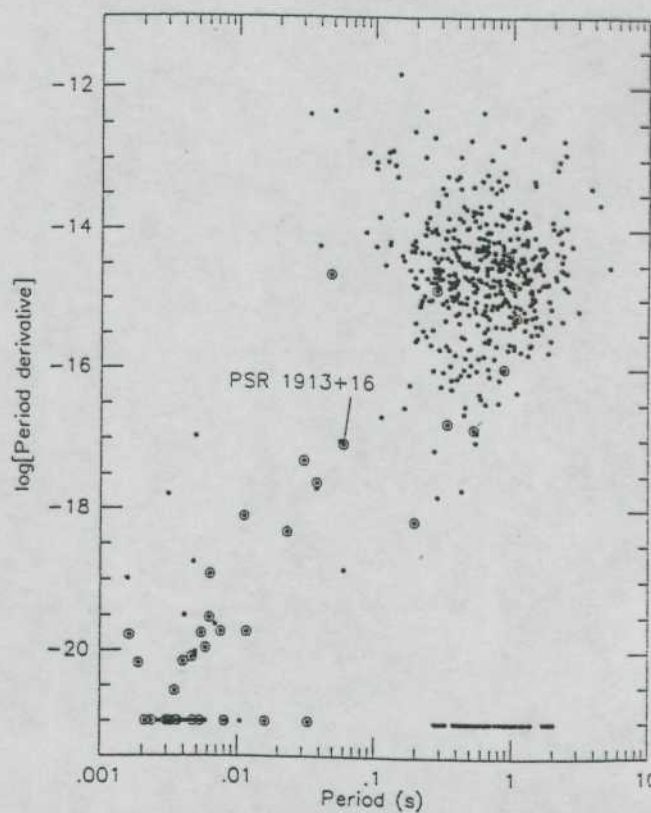
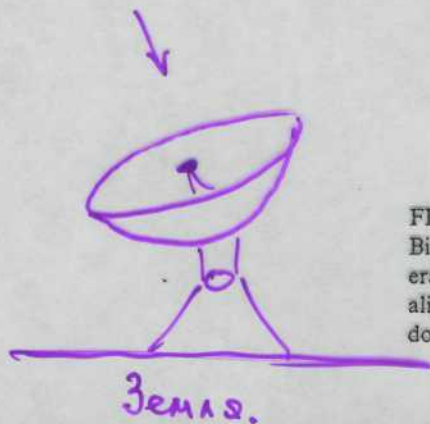


FIG. 2. Periods and period derivatives of known pulsars. Binary pulsars, denoted by larger circles around the dots, generally have short periods and small derivatives. Symbols aligned near the bottom represent pulsars for which the slow down rate has not yet been measured.



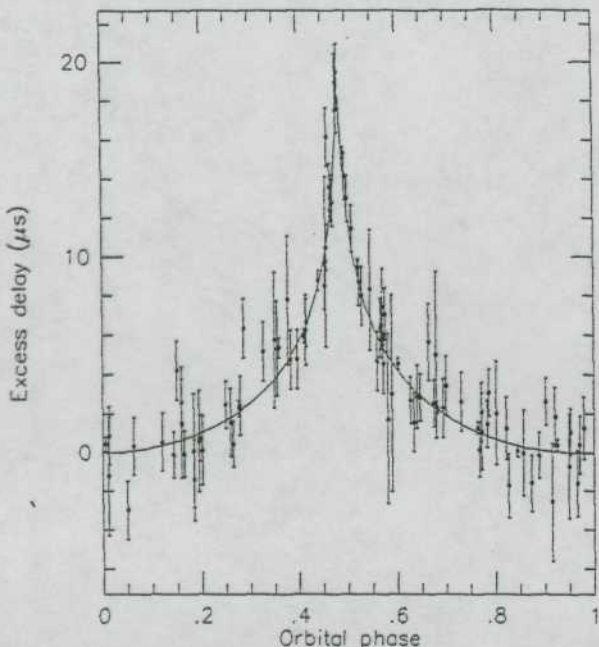


FIG. 8. Measurements of the Shapiro time delay in the PSR 1855+09 system. The theoretical curve corresponds to Eq. (10), and the fitted values of  $r$  and  $s$  can be used to determine the masses of the pulsar and companion star.

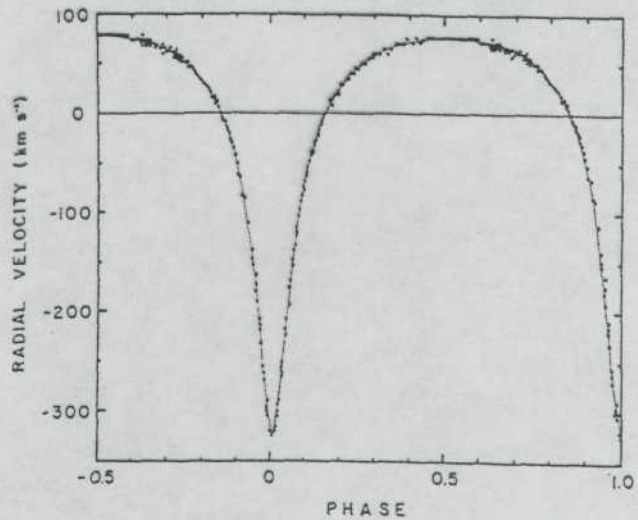
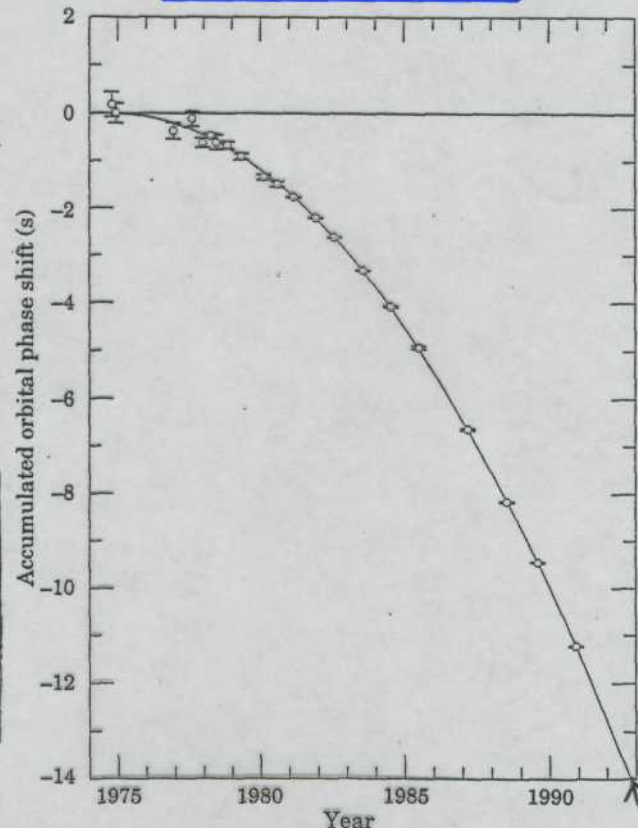


FIG. 12. The complete velocity curve for PSR 1913+16 from the discovery paper, fitted with a Keplerian orbital solution. The orbital phase is the fraction of a binary orbital period of  $7^h45^m$  (from R. A. Hulse and J. H. Taylor, 1975a).

PSR 1913 + 16



Accumulated shift of the times of periastron passage in the PSR 1913+16 system, relative to an assumed orbit with a constant period. The parabolic curve represents the general relativistic prediction, modified by Galactic effects, for orbital period decay from gravitational radiation damping forces.

(H3-H3)

360° - 100 лет

0.01° - 100 лет


Меркурий

• ОТО проверена  
с точностью  $10^{-3}$   
в сильных полях.

[ R.A. Huls, Rev. Mod. Phys.  
66, 699 (1994)  
J.H. Taylor, Rev. Mod. Phys.  
66, 711 (1994) ]

Нобелевская  
премия  
1993 г.

## Изложение ОТО:

1. Эквивалентность НСО и гравитации (лифт Эйнштейна)
2. Неевклидовость геометрии в НСО.
3.  $\Rightarrow$  гравитация искривляет пространство делая его неевклидовым.
4. Понятие геодезической. Кривизна прост-ва   
 $\Sigma, -\pi = c \delta\alpha$ ;  $c = \frac{1}{a^2}$ ;  $a$  — радиус крив-ти
5. Тензор Римана. (геометрическое интер-мд.)
6. Локальное устранение гравитации выбором касательной. НСО., но в соседней точке она есть  
При переходе от точки к точке поворот касательного вектора даёт Тензор Римана,  $R$
7. Эквивалентность инертной и гравитационной массы  
Тензор энергии-импульса
8. Уравнение ОТО.
9. Решение в Сферич-м мет-м случае. Метрика Шварц-шильда. Гравит-ый радиус. Задержание времени в грав-м. горизонт событий.